Interaction of internal solitary waves with long periodic waves within the rotation modified Benjamin–Ono equation

Interaction of internal solitary waves with long periodic waves within the rotation modified Benjamin–Ono equation

R.H.J. Grimshaw[a,b], N.F. Smyth[c,d] and Y.A. Stepanyants[b,e*)]

[a] Department of Mathematics, University College London, Gower Street, London, WC1E 6BT, UK;
[b] School of Sciences, University of Southern Queensland, Toowoomba, QLD, 4350, Australia;
[c] School of Mathematics, University of Edinburgh, James Clerk Maxwell Building, The King's Buildings, Peter Guthrie Tait Road, Edinburgh, Scotland, EH9 3FD, UK;
[d] School of Mathematics and Applied Statistics, University of Wollongong, Northfields Avenue, Wollongong, NSW 2522, Australia;
[e] Department of Applied Mathematics, Nizhny Novgorod State Technical University n.a. R.E. Alekseev, Nizhny Novgorod, Russia.

Abstract

The interaction of a solitary wave with a long background periodic wave in a deep ocean is studied within the framework of the rotation modified Benjamin–Ono equation. Using a multiple scales analysis, we find stationary and nonstationary solutions for a Benjamin–Ono soliton trapped within a long sinusoidal wave. We show that the radiation losses experienced by the soliton and caused by the Earth's rotation can be compensated by energy pumping from the background wave. However, the feedback of the soliton on the background wave eventually leads to the destruction of the coherent structure and energy dispersion in a quasi-random wave field. Estimates of the characteristic parameters of the soliton dynamics are presented for real oceanic conditions.

Keywords: Rotating fluid; Internal wave; Benjamin–Ono equation; Soliton; Asymptotic theory; Energy balance; Numerical modelling.

*) The corresponding author: Yury.Stepanyants@usq.edu.au

1. Introduction

In the paper by Ostrovsky & Stepanyants [1] the interaction of solitary waves with background long waves in the rotation modified Korteweg–de Vries (KdV) equation (alias the Ostrovsky equation) was studied. It was shown using an asymptotic analysis and numerical modelling that despite the "antisoliton theorem" [2, 3] that prohibits the existence of stationary localised solitary waves, such solitary waves can exist on a variable background. The study undertaken in [1] pertained to shallow water basins for which the characteristic width of the solitary wave is greater than the water depth. However, in the real deep ocean the situation often occurs for which a pycnocline (a sharp density interface) exists at a depth h much less than the total ocean depth H, $h << H$. Weakly nonlinear internal waves whose length is much greater than h can be described by the Benjamin–Ono (BO) equation [4, 5]. This equation, as for the KdV equation, is completely integrable and possesses solitary wave solutions known as algebraic BO solitons. In this paper we consider the dynamics of a BO soliton riding on a long background wave as governed by the rotation modified BO equation which was derived in [6]. In dimensional variables the basic equation is

$$\frac{\partial}{\partial x}\left(\frac{\partial \upsilon}{\partial t} + c_0 \frac{\partial \upsilon}{\partial x} + \alpha \upsilon \frac{\partial \upsilon}{\partial x} + \frac{\beta}{\pi} \frac{\partial^2}{\partial x^2} \wp \int_{-\infty}^{+\infty} \frac{\upsilon(\xi,t)}{\xi - x} d\xi \right) = \gamma \upsilon , \tag{1}$$

where the coefficients c_0, α, β, and γ depend on the environmental parameters (background stratification, water depth, etc.). In particular, in a density stratified fluid with the density $\rho_0(z)$ varying in the upper layer $-d < z < 0$ and an infinitely deep lower layer of constant density ρ_1, the coefficients in Eq. (1) can be determined through the modal function $\varphi(z)$ which describes the velocity potential. As was shown in [6], the modal function $\varphi(z)$ satisfies the Sturm–Liouville equation in the upper layer

$$c_0^2 \frac{d}{dz}\left(\rho_0(z) \frac{d\varphi}{dz} \right) + \rho_0(z) N^2(z) \varphi = 0 , \tag{2}$$

with the boundary conditions:

$$c_0^2\, d\varphi/dz = g\varphi, \quad \text{at} \quad z = 0; \qquad \text{and} \qquad d\varphi/dz = 0, \quad \text{at} \quad z = -d\,, \tag{3}$$

where $N^2(z) = -(g/\rho_0)(d\rho_0/dz)$ is the squared Brunt–Väisälä frequency.

Without loss of generality, we can set $\varphi(z = -d) = 1$. Then the coefficients of Eq. (1) are

$$\alpha = \frac{3}{I}\int_{-d}^{0} \rho_0(z) c_0^2 \left(\frac{d\varphi}{dz}\right)^3 dz; \quad \beta = \frac{\rho_1 c_0^2}{I}\varphi^2(-d); \quad I = 2\int_{-d}^{0} \rho_0(z) c_0 \left(\frac{d\varphi}{dz}\right)^2 dz; \quad \gamma = \frac{f^2}{2c_0},$$

where $f = 2\Omega\cos\phi$ is the Coriolis parameter, Ω is the frequency of Earth's rotation and ϕ is the geographic latitude.

If the density is constant in each of the upper and lower layers, but experiences a jump at the interface between the layers, then the coefficients are

$$c_0 = \sqrt{\frac{\rho_1 - \rho_0}{\rho_0} gh}; \quad \alpha = -\frac{3}{2}\frac{c_0}{h}; \quad \beta = \frac{\rho_1}{\rho_0}\frac{c_0 h}{2}; \quad \gamma = \frac{f^2}{2c_0}. \tag{4}$$

For perturbations with infinitesimal amplitudes, so that $\upsilon \sim \exp[i\,(\omega t - kx)]$, we obtain from equation (1) the dispersion relation

$$\omega = c_0 k - \beta k|k| + \frac{\gamma}{k}; \quad c_p \equiv \frac{\omega}{k} = c_0 - \beta|k| + \frac{\gamma}{k^2}; \quad c_g \equiv \frac{d\omega}{dk} = c_0 - 2\beta|k| - \frac{\gamma}{k^2}, \tag{5}$$

where c_p and c_g are the phase and group velocities, respectively.

Equation (1) is, apparently, non-integrable, and its solutions are not known in analytic form thus far. Particular numerical and approximate solutions describing adiabatic soliton decay under the influence of various dissipative mechanisms were obtained in [7]. Because Eq. (1) is very similar to the Ostrovsky equation, one can expect that it can possess stationary solutions representing, in particular, a solitary wave riding on the crest or trough of a long background wave; such solutions were obtained for the Ostrovsky equation in [8–10]. As was shown in [11], if the amplitude of a solitary wave is not properly matched with the amplitude of the background wave, then the solitary wave can travel along the long wave, periodically accelerating and decelerating,

growing and decaying. The solitary wave can also be trapped within the periodic background wave and oscillate around an equilibrium state near the trough of the background wave [1].

In this sequel we use a multiple scales analysis to describe the dynamics of a BO algebraic soliton on a long background wave. The background wave is taken as one of the particular solutions of the reduced rotation modified BO equation (1) with $\beta = 0$. As shown in [12–16], there exists a family of exact periodic solutions of the reduced equation. After presenting general relationships in Sec. 2, we consider solitary wave interaction with a periodic background wave in Sec. 3. Then, in Sec. 4 we present the results of direct numerical simulations of solitary wave interaction with a periodic background wave and discuss the results obtained in Sec. 5.

2. Interaction of a solitary wave with a long background wave.

Solutions of the rotation modified BO equation (1) critically depend on the relative sign of the dispersion coefficients β and γ. Similarly, to the Ostrovsky equation, it can be proved that for $\beta\gamma > 0$ (the "oceanic case"), localised solitary waves do not exist [2, 3]. In the opposite case $\beta\gamma < 0$, the "antisoliton theorem" does not hold and solitary waves, apparently, can exist. In this paper we will consider only the usual oceanic case with $\beta\gamma > 0$.

Equation (1) is, as far as is known, nonintegrable, but it possesses at least two integrals of motion. One of them is the "zero mass" integral

$$M \equiv \int \upsilon(x,t)dx = 0\,. \tag{6}$$

The integration here is taken either over the wave period for periodic waves, or over the entire x-axis for localised solutions. When there is no rotation, $\gamma = 0$, the BO equation possesses an infinite number of integrals of motion [17] and the "wave mass" integral M can be an arbitrary constant which is determined by the initial conditions. In our case, Eq. (6) is not just an integral of motion, but rather a constraint which demands that initial conditions must be consistent with the zero-mass condition.

To proceed further, it is convenient to reduce Eq. (1) to dimensionless form by means of the transformations

$$x' = \left(\frac{\gamma}{\beta}\right)^{1/3}(x - c_0 t), \quad t' = \beta\left(\frac{\gamma}{\beta}\right)^{2/3} t, \quad u = \frac{\alpha}{\beta}\left(\frac{\beta}{\gamma}\right)^{1/3} \upsilon. \tag{7}$$

Then, Eq. (1) can be written as (the primes on the new variables x and t are omitted from now on):

$$\frac{\partial}{\partial x}\left(\frac{\partial u}{\partial t} + u\frac{\partial u}{\partial x} + \frac{1}{\pi}\frac{\partial^2}{\partial x^2}\wp\int_{-\infty}^{+\infty}\frac{u(\xi,t)}{\xi - x}d\xi\right) = u. \tag{8}$$

Following Ref. [1], we seek a solution of this equation in the form $u(x, t) = u_1(x, t) + u_2(x, t)$, where $u_1(x, t)$ is a smooth periodic background wave with wavelength Λ and $u_2(x, t)$ is a representation of a perturbed BO soliton with slowly varying amplitude and width (see below). If the characteristic soliton width Δ is much smaller than the wavelength Λ of the background wave, the equations for these components can be approximately separated. First, we assume that the function $u_1(x, t)$ is given, that is $u_1 = u_1(s = x - ct)$, where c is a constant wave speed. For our present purposes we assume that this periodic wave is a long wave and so the linear dispersive term due to the integral in Eq. (8) can be omitted. It then satisfies the reduced Ostrovsky equation (see, for example, [12, 16] and references therein):

$$\frac{d^2}{ds^2}\left(\frac{1}{2}u_1^2 - cu_1\right) = u_1. \tag{9}$$

The shape of the stationary solution $u_1(s)$ can vary from a small amplitude sinusoidal wave to a limiting periodic wave in the form of a sequence of parabolic arcs, as shown in Fig. 1 [12–16]; all waves of this family have zero mean value.

As mentioned above, we intend that $u_2(t, x)$ in the trial solution describes a relatively narrow BO soliton with a characteristic width $\Delta << \Lambda$, which in the asymptotic limit when rotation is ignored satisfies Eq. (8) with a zero right hand side. To derive the equation for the evolution of $u_2(t, x)$ under the influence of rotation, we first change the reference frame to $s = x - ct$, so that Eq. (8) becomes:

$$\frac{\partial u_2}{\partial t}+\left[u_1(s)-c\right]\frac{\partial u_2}{\partial s}+u_2\frac{\partial u_2}{\partial s}+\frac{1}{\pi}\frac{\partial^2}{\partial s^2}\wp\int_{-\infty}^{+\infty}\frac{u_2(\xi,t)}{\xi-s}d\xi=-\int_s^{\infty}u_2(\xi,t)d\xi-\frac{du_1}{ds}u_2. \qquad (10)$$

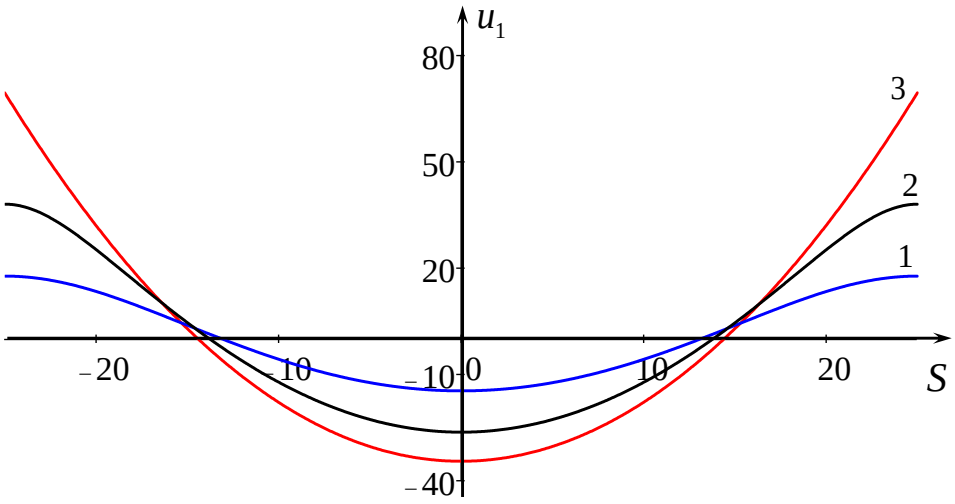

Fig. 1. (colour online). A family of zero-mass stationary periodic solutions of the reduced Ostrovsky equation (9) with $\Lambda = 50$. Line 1 pertains to quasi-sinusoidal wave with $c = 64$, line 2 illustrates a nonlinear wave with $c = 66$, and line 3 represents a periodic sequence of parabolic arcs with $c = (25/3)^2 \approx 69.4$.

We further assume that the solitary wave is localised at a location $s = S(t)$ and rewrite Eq. (10) as:

$$\frac{\partial u_2}{\partial t}+\left[u_1(S)-c\right]\frac{\partial u_2}{\partial s}+u_2\frac{\partial u_2}{\partial s}+\frac{1}{\pi}\frac{\partial^2}{\partial s^2}\wp\int_{-\infty}^{+\infty}\frac{u_2(\xi,t)}{\xi-s}d\xi$$

$$=-\int_s^{\infty}u_2(\xi,t)d\xi-\frac{\partial}{\partial s}\left\{\left[u_1(s)-u_1(S)\right]u_2\right\}. \qquad (11)$$

For a relatively short solitary wave the right hand side of this equation can be treated as a small perturbation. When this term is neglected, Eq. (11) has the exact soliton solution:

$$u_2=\frac{A}{1+\left[(s-S)/\Delta\right]^2}, \qquad (12)$$

where $\Delta = 4/A$ and

$$\frac{dS}{dt}=u_1(S)-c+\frac{A}{4}. \qquad (13)$$

When this solitary wave travels along the background long wave its amplitude A slowly varies with time. To derive an equation for the amplitude variation, one can use one of the known regular

asymptotic methods, described, for instance, in [18–21]. Here we use an alternative simplified approach similar to that developed in [22] for the description of KdV solitary wave interaction with a sinusoidal pump wave in an electro-magnetic transmission line. This approach is based on a phase and energy balance.

The equation for the solitary wave amplitude follows from the energy balance equation [19, 20]. Multiplying Eq. (11) by u_2 and integrating over s within the interval $[-L/2, L/2]$ in the vicinity of soliton maximum, where $\Delta << L << \Lambda$, we obtain (cf. [1]):

$$\frac{d}{dt}\int_{-L/2}^{L/2} u_2^2 ds \approx -\left(\int_{-L/2}^{L/2} u_2 ds\right)^2 - 2\frac{du_1}{ds}\int_{-L/2}^{L/2} u_2^2 ds. \tag{14}$$

Here, it has been taken into account that the gradient of the background wave du_1/ds is approximately constant in the neighbourhood of the solitary wave, whose field rapidly decays away from its centre, so that $u_2(\pm L/2) \approx 0$ (i.e., one can set $L = \infty$). Substituting the soliton solution (12) for $u_2(t, x)$, after integration we obtain:

$$\frac{dA}{dt} = -8\pi - A\frac{du_1(s)}{ds}\bigg|_{s=S(t)}. \tag{15}$$

The set of equations (13) and (15) defines the variation of the amplitude A and phase S with time. To get some insight into the possible effects, we consider below only the limiting cases of a background small amplitude sinusoidal wave.

3. Interaction of a BO solitary wave with a sinusoidal wave

Let us assume that the long background wave is sinusoidal, so that

$$u_1(s) = U_0 \sin\left(ks - \frac{\pi}{2}\right) \tag{16}$$

with period $\Lambda = 2\pi/k$, amplitude $U_0 << U_{lim} \equiv \Lambda^2/36$ and phase speed $c = 1/k^2$. The restriction on the wave amplitude follows from a comparison with the amplitude of a limiting wave as represented by a sequence of parabolic arcs, as shown in Fig. 1. The phase speed of the sinusoidal

wave follows from linearizing Eq. (8) when both the nonlinear term and the second order derivative are neglected.

3.1 The conservative case

Consider first the solitary wave dynamics on a variable background field, ignoring the effect of radiative losses which the solitary wave experiences due to the influence of large scale dispersion. The effect of such radiation has been studied by Grimshaw et al. [7], who showed that in finite time a BO soliton experiences terminal decay, when it transforms to a radiating wavetrain (a similar process has been studied for the KdV soliton within the framework of the Ostrovsky equation [18]).

Here, we study the influence of the background wave on the dynamics of a solitary wave based on neglecting the associated radiative losses, but do not deal with the feedback of the solitary wave on the background wave. Substituting the solution (16) for the background wave $u_1(S)$ into Eqs. (13) and (15), and omitting the radiative loss term, -8π in Eq. (15), we obtain a set of two equations for S and A

$$\frac{dS}{dt} = \frac{A}{4} - U_0 \cos kS - \frac{1}{k^2}, \tag{17}$$

$$\frac{dA}{dt} = -AU_0 k \sin kS. \tag{18}$$

This system is conservative with the Hamiltonian $H(A, S)$

$$H(A,S) = \frac{A^2}{8} - AU_0 \cos kS - \frac{A}{k^2}, \tag{19}$$

which is a conserved quantity. Here, $S = 0$ corresponds to one of the troughs of the background wave, playing the role of an energy pump for the solitary wave. We consider first the stationary points of this dynamical system. In general, there are four such points within each period of the sinusoidal wave

$$A_1 = 4\left(\frac{\Lambda^2}{4\pi^2} + U_0\right), \quad S_1 = 0 \pm n\,\Lambda; \tag{20}$$

$$A_2 = 4\left(\frac{\Lambda^2}{4\pi^2} - U_0\right), \quad S_2 = -\Lambda/2 \pm n\,\Lambda. \tag{21}$$

$$A_{3,4} = 0, \quad kS_{3,4} = \cos^{-1}(-1/k^2 U_0). \tag{22}$$

Here, n is an integer. Two of these stationary points, $A_{1,2}$, correspond to solitary waves of non-zero amplitude. We see from (21) that the amplitude A_2 exists only for $\Lambda^2/U_0 > (2\pi)^2$. Solutions with zero amplitude cannot be considered here, because for such solitons the characteristic widths become infinite; this violates our assumption $\Delta << \Lambda$ or $A >> 4/\Lambda$. Figure 2 illustrates stationary solitary waves riding on the sinusoidal background wave. Solitons marked by numbers 2 and 2′ in the right-hand side of the figure belong to the next period. In particular, the solitons marked by the numbers 1 and 2 correspond to stationary points in the phase plane of Fig. 3 (and are marked by red dots).

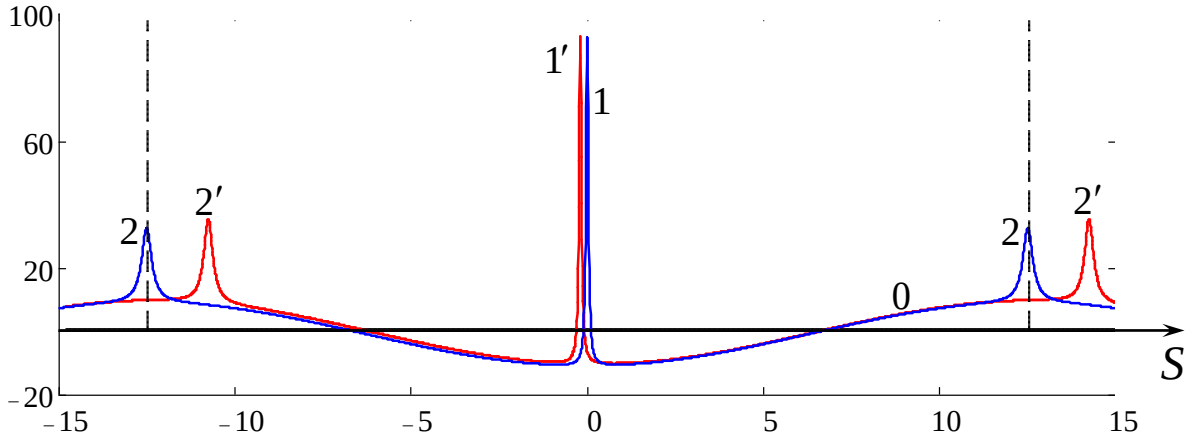

Fig. 2 (colour online). One spatial period of the background sinusoidal wave (12) with $\Lambda = 25$ and amplitude $U_0 = 10$ (line 0) with the BO solitons sitting on the troughs (1) and on the crests (2). Lines 1′ and 2′ pertain to stationary solitons with the radiative losses (see below). Vertical dashed lines show the period of the background wave.

The phase portraits are then given by $H(A, S)$ = constant, which can be evaluated at the point $A = A_0$, $S = S_0$, and are shown in Fig. 3. There is a family of closed trajectories describing solitary wave oscillations in the potential well of the background wave around its minima. There is also a

family of open trajectories describing solitary waves travelling along the background wave, either in the same direction as the background wave (the trajectories above line 1), or in the opposite direction (the trajectories below line 2 which are not shown). The separatrix consisting of two branches (lines 1 and 2) describes a solitary wave which travels from one crest of the background wave to another one. One of the stationary points (20) of centre type is located at $S = 0$, i.e. in the trough of the background wave. The stationary points (21) of saddle type shown in the corners of the separatrices 1 and 2, at $S = \Lambda/2$, correspond to unstable equilibrium positions on the wave crests.

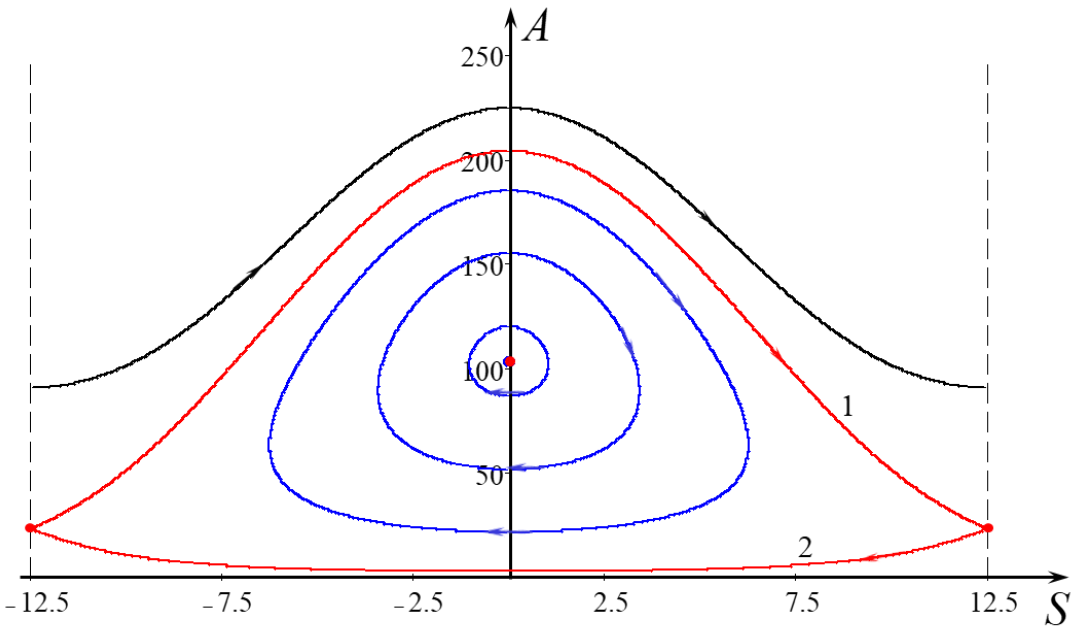

Fig. 3 (colour online). The phase portrait of the dynamical system (17), (18) in the conservative case with $\Lambda = 25$, $U_0 = 10$. Lines 1 and 2 are the separatrices. Vertical dashed lines show the boundary of one cell of the phase portrait which is periodic in the horizontal direction.

The period of oscillation around the central point can be easily estimated for relatively small amplitude oscillations. It follows from the dynamical system (17) and (18) linearized around the equilibrium state (19) that the period of oscillation is

$$T = \frac{2\pi\Lambda}{\sqrt{U_0\left(\Lambda^2 + 4\pi^2 U_0\right)}}. \qquad (23)$$

Substituting $\Lambda = 25$ and $U_0 = 10$, as in Fig. 3, we obtain $T \approx 1.56$.

3.2 Influence of radiative losses on soliton dynamics

Now, let us take into consideration the radiative losses which the BO soliton experiences due to the rotational effect [7]. In the case of a sinusoidal background wave, Eq. (18) is replaced by

$$\frac{dA}{dt} = -AU_0 k \sin kS - 8\pi. \tag{24}$$

Although the set of equations (17) and (24) is not energy conserving, there is a Hamiltonian-like conserved quantity $H_{rl}(A, S)$ given by

$$H_{rl}(A,S) = \frac{A^2}{8} - AU_0 \cos kS - \frac{A}{k^2} - 8\pi S\,. \tag{25}$$

As before, the phase portrait is obtained from $H_{rl}(A, S)$ = constant and is shown in Fig. 4.

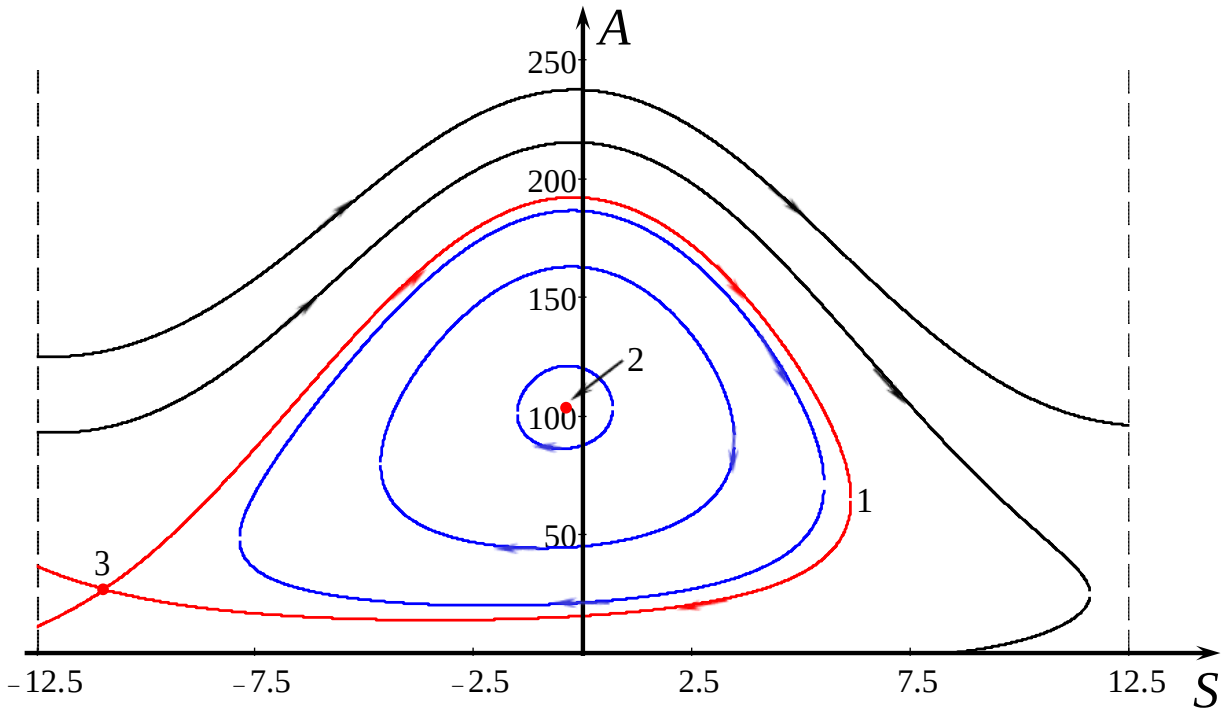

Fig. 4 (colour online). The phase portrait of the dynamical system (17), (24). Line 1 is the separatrix separating closed and unclosed trajectories. Points 2 and 3 represent equilibrium states; corresponding soliton solutions are shown in Fig. 2 by pulses labelled by the numbers 1′ and 2′. Vertical dashed lines show the boundaries of the main cell.

In contrast to the Ostrovsky equation [1], the dynamical system (17) and (24) is quasi-conservative. All its solutions corresponding to trajectories outside of the separatrix 1 in Fig. 4 eventually decay and vanish, although before vanishing the soliton amplitude can oscillate with S and travel from one cell of the phase plane to another. This corresponds to a BO solitary wave travelling on a sinusoidal background wave until it arrives in a certain period where it quickly decays (one of such solutions corresponds to the trajectory which touches the horizontal axis and stops near S =7.5 in Fig. 4). Otherwise, all trajectories within the separatrix are closed and represent periodic oscillations around the equilibrium point 2 in Fig. 4, as for the conservative case.

The equilibrium points of the dynamical system (17) and (24) can be found by setting the time derivatives to zero. Then, after some manipulation, we obtain the equation

$$\tan^4\frac{kS}{2}+\frac{kU_0^2}{\pi}\left(\frac{1}{k^2U_0}-1\right)\tan^3\frac{kS}{2}+2\tan^2\frac{kS}{2}+\frac{kU_0^2}{\pi}\left(1+\frac{1}{k^2U_0}\right)\tan\frac{kS}{2}+1=0\,. \tag{26}$$

which determines S. It can be shown that this quartic polynomial with respect to $\tan(kS/2)$ has only two real roots, which can be found analytically, in principle, but it is easier to find them numerically. Once these roots S_{eq} are determined, one can find from Eq. (17) with zero left hand side the soliton amplitude

$$A_{eq}=4\left(U_0\cos kS_{eq}+\frac{1}{k^2}\right). \tag{27}$$

Two equilibrium points are shown in Fig. 4 for U_0 = 10 and $\Lambda = 2\pi/k$ = 25. They are A_1 = 103.13, S_1 = –0.39 (see point 2 in Fig. 4) and A_2 = 26.32, S_2 = –10.95 (see point 3 in Fig. 4). The former one is a centre, whereas the latter is a saddle. There is one trajectory in each cell which originates at the saddle point 3, makes a loop around the centre and then returns back to the saddle in infinite time. Such a trajectory corresponds to an unstable solitary wave solution.

The quartic polynomial (26) has real roots only if $U_0 \geq U_{cr} = 4\pi^2/\Lambda$. Therefore, two equilibrium positions can exist when this condition holds. When U_0 approaches the critical value from the top, the solitary wave amplitudes become equal and their equilibrium positions coincide

at $S_{eq} = -\Lambda/4$ where the gradient of the background wave is maximal. In this position the energy pumping to the solitary waves from the sinusoidal background wave is maximal and compensates the radiative energy losses.

Figure 2 shows stationary solitary waves riding on a background sinusoidal wave of the same amplitude $U_0 = 10$, but with radiative losses taken into account. Soliton 1′ is in the stable position and soliton 2′ is in the unstable (saddle type) position. As compared with the conservative case, the unstable solitary wave shifts forward from the crest and thus its phase becomes slightly greater than $\Lambda/2$, whereas the stable solitary wave shifts backwards from the trough and its phase becomes slightly negative. This is caused by energy exchange with the background wave as only on the negative (frontal) slope of the sinusoidal wave can a solitary wave acquire energy from the background wave to compensate its energy loss due to radiation.

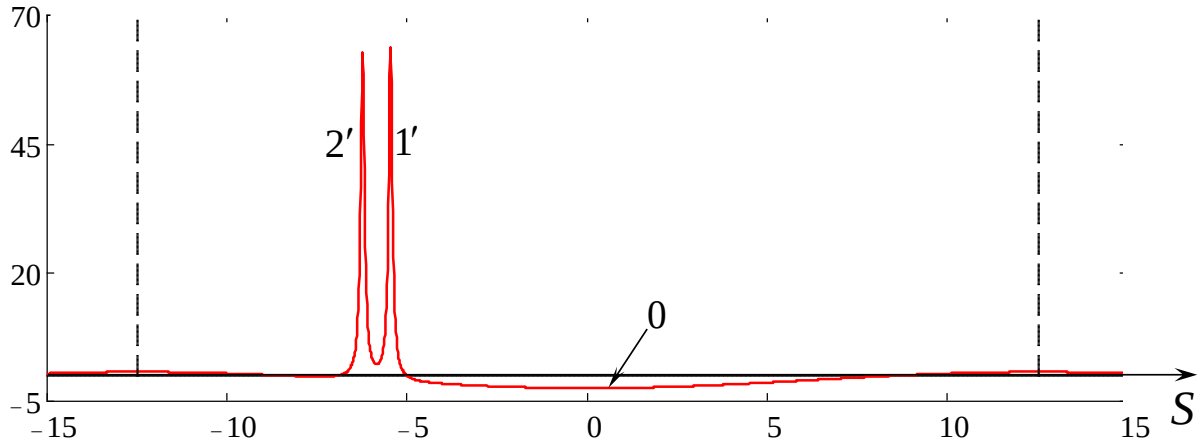

Fig. 5 (colour online). One spatial period of the background sinusoidal wave (16) with $\Lambda = 25$ and amplitude $U_0 = 1.58$ (line 0) with the BO solitary waves sitting at the equilibrium positions when the radiative losses are taken into account. Vertical dashed lines show the period of the background wave.

In Fig. 5 we show the near-critical situation for which two solitary waves with the radiative effect taken into account ride on a sinusoidal wave of the small amplitude $U_0 = 1.58$. In such a situation when the solitary waves are very close to each other the interaction between them needs to be taken into account. This leads to further complication of the description of the soliton

dynamics (more details can be found in [23] for two KdV solitary waves interacting with a periodic background wave as governed by the Ostrovsky equation).

In Fig. 6 we illustrate the dependence of the stationary solitary wave amplitudes on the amplitude of the background sinusoidal wave for $\Lambda = 25$. The dashed lines 1 and 2 refer to the conservative case, as in Eqs. (20) and (21) for solitary waves propagating on the troughs and crests, respectively. Lines 3 and 4 correspond to the case for which radiative losses are taken into account. In this case stationary solitary waves can exist only when the amplitude of the background wave is large enough, $U_0 \geq U_{cr} = 4\pi^2/\Lambda$. At critically solitary waves with equal amplitudes formally are located at $S_{eq} = -\Lambda/4$ where the background wave gradient is maximal (see Fig. 7). The value of the carrier wave amplitude shown in Fig. 5 is $U_0 = 1.58$ that is slightly greater than U_{cr}; therefore, the positions of two stationary solitons are very close S_{eq}. When U_0 increases above the critical value U_{cr}, lines 3 and 4 rapidly approach the asymptotic lines 1 and 2 which represent solitary wave amplitudes $A_{1,2}$ for the conservative case, as in Eqs. (20) and (21).

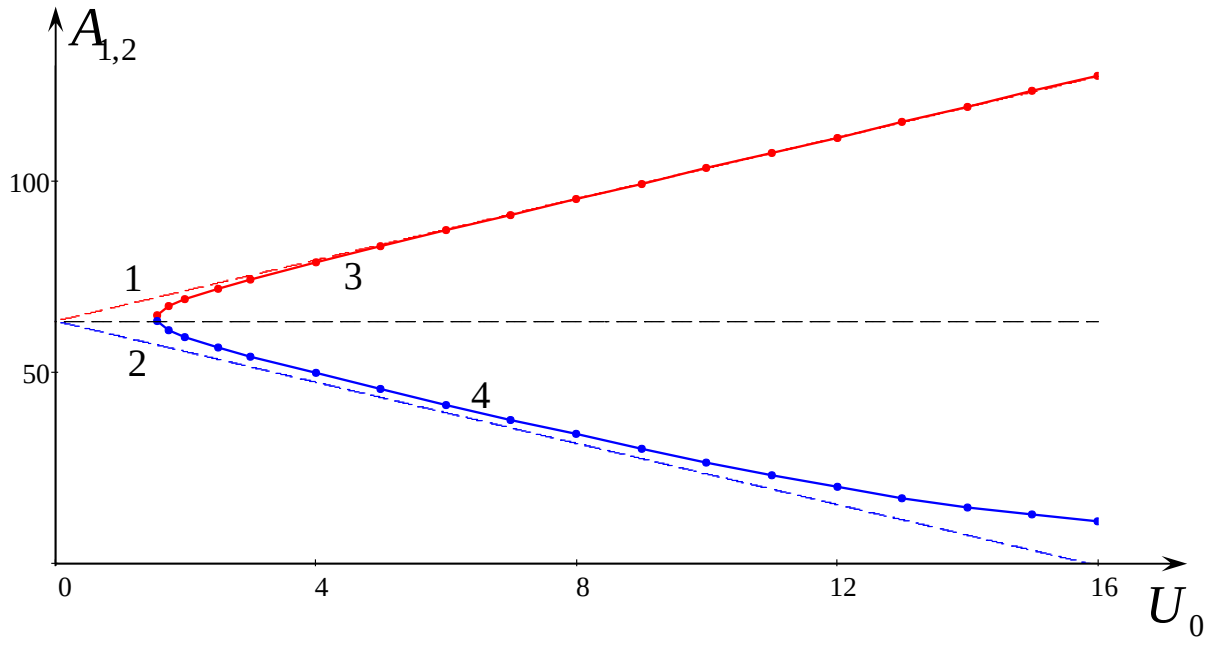

Fig. 6 (colour online). Stationary solitary wave amplitudes versus the amplitude of the background sinusoidal wave for $\Lambda = 25$ in the conservative case (lines 1 and 2) and when the radiative losses are taken into account (lines 3 and 4). Lines 1 and 3 pertain to solitary waves sitting in the troughs, and lines 2 and 4 to the solitary waves sitting on the crest.

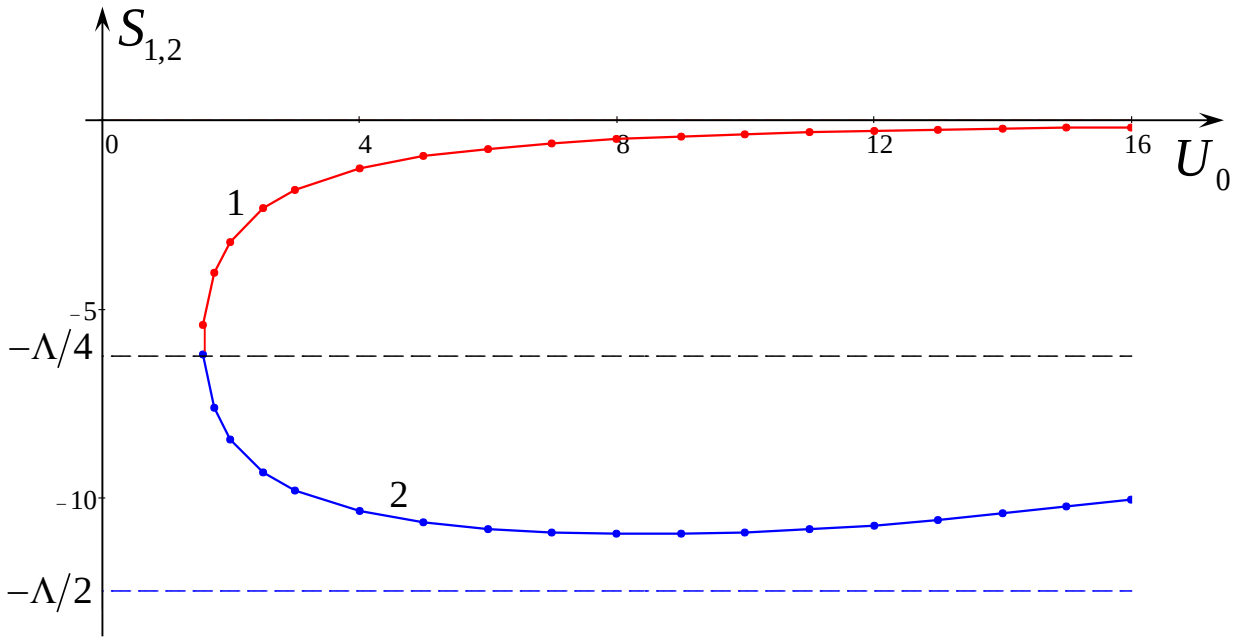

Fig. 7 (colour online). Positions of stationary solitons on the background sinusoidal wave against the amplitude U_0 for $\Lambda = 25$. Line 1 pertains to the soliton sitting next to the trough, and line 2 to the soliton sitting next to the crest. In the conservative case they would be sitting at $S = 0$ and $S = \Lambda/2$ respectively.

The stationary positions of solitary waves on the background wave which are determined by the roots of the quartic polynomial (26) are shown in Fig. 5 in terms of the dependences $S_{1,2}$ against U_0 for $\Lambda = 25$. The solutions shown in Figures 6 and 7 are valid for amplitudes $U_0 << U_{lim} \equiv \Lambda^2/36$ (see after Eq. (16)); in this particular case $\Lambda = 25$, $U_{lim} = (25/6)^2 \approx 17.36$.

The theory developed so far describes the basic effects of the interaction between a solitary wave and a long sinusoidal wave. The main consequence is that, unlike the case of solitary wave non-existence for a homogeneous background, a solitary wave can exist and be stable on a long wave since the pumping of energy from the background wave can compensate radiative losses. At the same time, there are various additional factors which were ignored so far. Below, we consider one of these factors, the feedback of a solitary wave on the background sinusoidal wave.

3.3 The feedback of a solitary wave on the background sinusoidal wave

In the above analysis the background wave was assumed as given. However, in reality, this wave undergoes attenuation due to energy consumption by the solitary wave, the energy of the

background wave changes at the same rate as it is consumed by the solitary wave riding on it. We assume that there is only one solitary wave riding in each period of the background wave, and neglect the direct interaction between the solitary waves. In this case the energy balance equation analogous to (14) is, as written for each period of the background wave

$$\frac{d}{dt}\int_{-\Lambda/2}^{\Lambda/2} u_1^2 ds = -\int_{-L/2}^{L/2} u_2^2 \frac{du_1}{ds} ds \approx -\frac{du_1}{ds}\int_{-L/2}^{L/2} u_2^2 ds. \tag{28}$$

On the right-hand side of this equation the derivative of $u_1(s)$ is taken at the location of a solitary wave $s = S(t)$. It can be considered as a constant here, because the solitary wave width is very small in comparison and its shape resembles a Dirac delta-function. Substituting the expressions (12) and (16) for u_2 and u_1, respectively, and integrating, we obtain the equation for the slowly varying amplitude of the background wave $U(t)$

$$\frac{dU}{dt} = Ak^2 \sin kS\,. \tag{29}$$

Now the set of three equations, (17), (24) and (29) is analysed, where in (17) and (24) we replace U_0 with $U(t)$. For convenience, we collect all three equations together as

$$\frac{dS}{dt} = \frac{A}{4} - U\cos kS - \frac{1}{k^2}, \tag{30}$$

$$\frac{dA}{dt} = -AUk\sin kS - 8\pi. \tag{31}$$

$$\frac{dU}{dt} = Ak^2 \sin kS\,. \tag{32}$$

This dynamical system of "1.5 degrees of freedom" has the first integral:

$$2\pi A(t) + \frac{1}{2}U^2(t)\Lambda = 2\pi A_0 + \frac{1}{2}U_0^2\Lambda - 16\pi^2 t\,, \tag{33}$$

where the left-hand side represents the total energy of the solitary wave (the first term) and one period of background sinusoidal wave (the second term). Equation (33) shows that the total energy of the wave field linearly decreases with time due to the radiation losses experienced by the solitary

wave. The solitary wave borrows energy from the background wave and radiates it away. If there is no background wave, we obtain form Eq. (33) the decay law of the soliton amplitude as previously derived in [7].

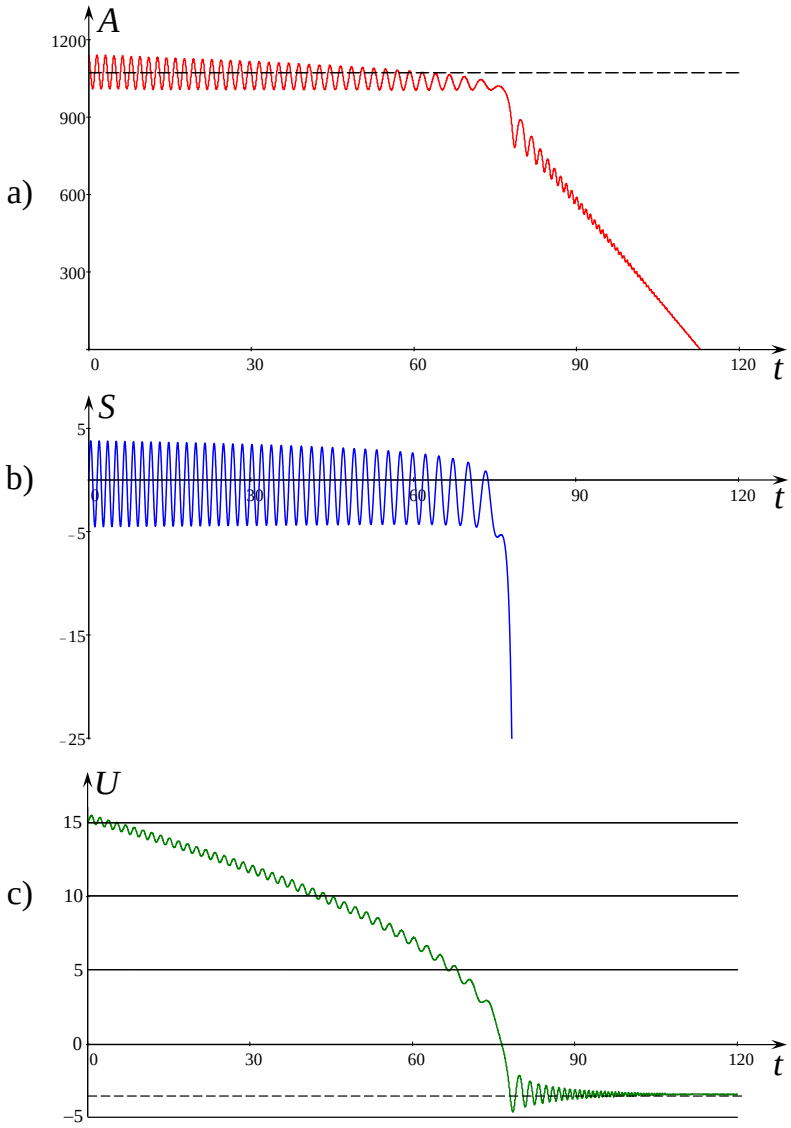

Fig. 8 (colour online). The dependences of the solitary wave amplitude $A(t)$ (frame a) and position $S(t)$ (frame b) on time. Dashed horizontal line in frame a) shows stationary solitary wave amplitude A_1 when the influence of solitary wave on the background wave is ignored. Frame c) shows the dependence of amplitude of the background sinusoidal wave on time. Dashed horizontal lines in this frame shows stationary amplitude of the sinusoidal wave when the solitary wave completely vanishes (the negative value implies that phase of sine wave was changed by π).

The dynamical system (30)–(32) is non-integrable, but can be easily investigated numerically. As follows from Eq. (33), the solitary wave amplitude in this case vanishes in a finite time which

depends on the initial conditions and there is no equilibrium state. An example of the numerical solution of the dynamical system (30)–(32) is shown in Fig. 8 for the initial condition $A_0 = 1140$, $S_0 = 0$, $U_0 = 15$ and $\Lambda = 100$. It can be seen that the solitary wave experiences a few oscillations around the trough of the background wave, then quickly decays linearly with time on average (see frame a). However, the solution becomes meaningless from a physical point of view when solitary wave amplitude approaches zero and its width increases without bound. The amplitude of the background wave decays as expected, changes its phase by π and eventually stabilises around the terminal value $|U_t| \approx 3.46$ (see the horizontal dashed line in frame c).

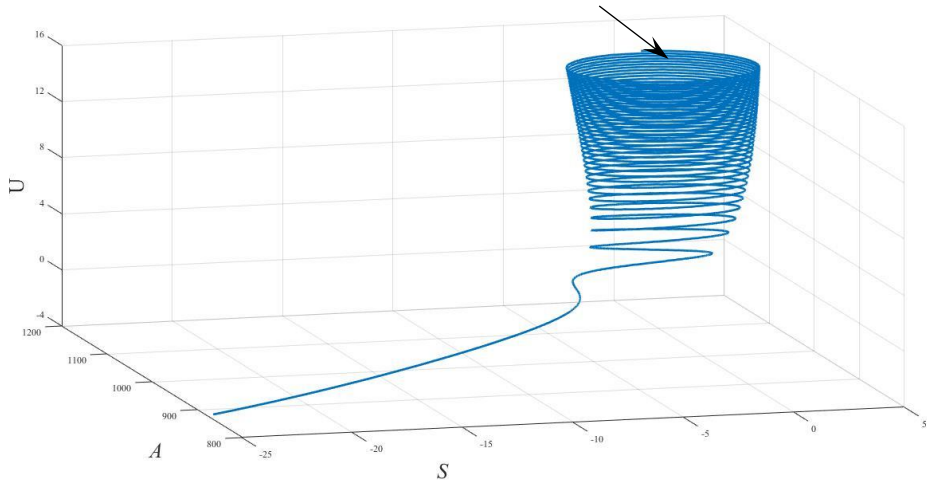

Fig. 9 (colour online). An example of the typical phase trajectory of the system (30)–(32) in 3D phase space for the particular initial condition: $U_0 = 15$, $A_0 = 1140$, $S_0 = 0$, and $\Lambda = 100$. Black arrow shows the starting point.

Figure 9 illustrates a typical phase trajectory in the three-dimensional phase space of the dynamical system (30)–(32). At the initial stage the solitary wave amplitude oscillates and decays within one period of the background wave and consumes energy to compensate the radiation losses, after which its amplitude rapidly decreases. The process of solitary wave decay can also be demonstrated on the phase plane which is a projection of the three-dimensional phase space of Fig. 9 onto the *SA*-plane, as shown in Fig. 10 by line 2. In the same figure we also show the phase

trajectory of the dynamical system (30) and (31) when the amplitude of the background sinusoidal wave is assumed constant and the influence of the solitary wave on the background wave is ignored (see line 1). In both cases for lines 1 and 2 the initial conditions are the same.

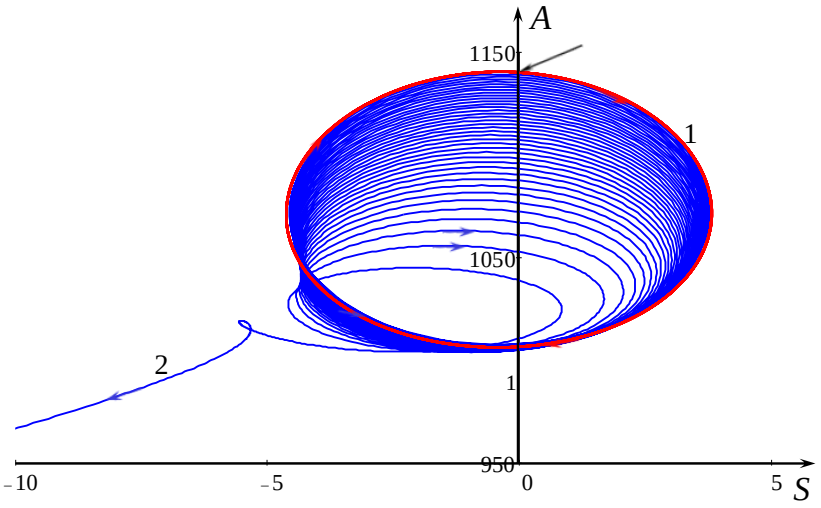

Fig. 10 (colour online). A projection of the typical phase trajectory shown in Fig. 9 onto the *SA*-plane. Black arrow shows the starting point. Line 1 represents the phase trajectory when the amplitude of background wave is fixed and line 2 is the phase trajectory when the amplitude of the background waves varies with time.

4. Numerical study

To validate the theoretical results described above we undertook direct numerical calculations of the soliton dynamics on the background of a sinusoidal wave within the framework of Eq. (1), where we set $c_0 = 0$ because the corresponding linear term can be removed by a Galilean transformation of the coordinates. The numerical method was based on the pseudo-spectral method of Fornberg and Whitham [24], as extended by Chan and Kerkhoven [25] to enhance stability at high wavenumbers (see [26]). Equation (8) is integrated in x to obtain a BO equation with the integral of u as a forcing. The dispersive term in Eq. (8) is easily calculated in Fourier space, as is the integral of u. The solution is then propagated forward in time in Fourier space using the fourth-order Runge–Kutta method. For this time equation the dispersive terms, based on the dispersion relation $\omega = -k|k|$, are incorporated into an integrating factor to enhance stability at high

wavenumbers [25]. The use of a pseudo-spectral method results in the periodic boundary conditions on the interval $x \in [0, \Lambda]$. The initial background wave was chosen as a sinusoidal wave with the amplitude $U_0 = 15$ and wavelength $\Lambda = 100$. A soliton with amplitude $A = 1140$ was then placed in the wave minimum (line 1 in Fig. 11). Figure 11 shows a fragment of the total wave field in the reference frame co-propagating with the background sinusoidal wave. In agreement with the theory, the soliton oscillates around the quasi-equilibrium position with a periodically varying amplitude. Due to the large solitary wave amplitude, the time step for the Runge–Kutta method needed to be small for stability, $dt = 5 \cdot 10^{-8}$, and the number of modes large for an accurate solution, $N = 2 \cdot 10^{18}$, resulting in very lengthy computation times. The net result was that the numerical solution was only found within one period of soliton oscillation around the equilibrium position in the trough of the background wave.

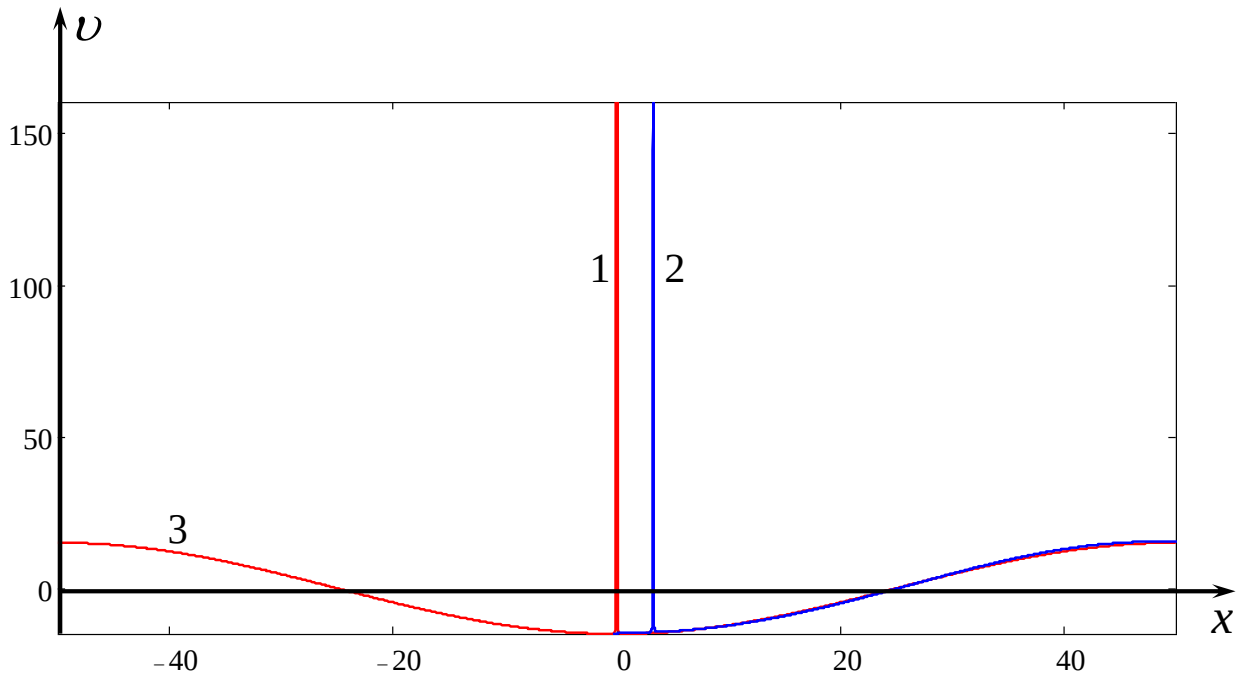

Fig. 11 (colour online). A fragment of numerical solution of Eq. (1). Line 1 – the initial BO soliton located in the trough of sinusoidal wave shown by line 3, line 2 – the same soliton at $t = 0.37$ shifted to the right in the coordinate frame co-moving with the sinusoidal wave. The tops of the solitons are cut.

The numerically calculated time dependence of the normalised soliton amplitude $A(t)/A(0)$ is shown in Fig. 12 by dots. For comparison the theoretical dependence, which is the same as in Fig. 8(a), but for a different time interval, is shown by the solid line 1. It can be seen that there is satisfactory agreement between the numerical data and the theoretical dependence, at least within the first period of the soliton oscillation.

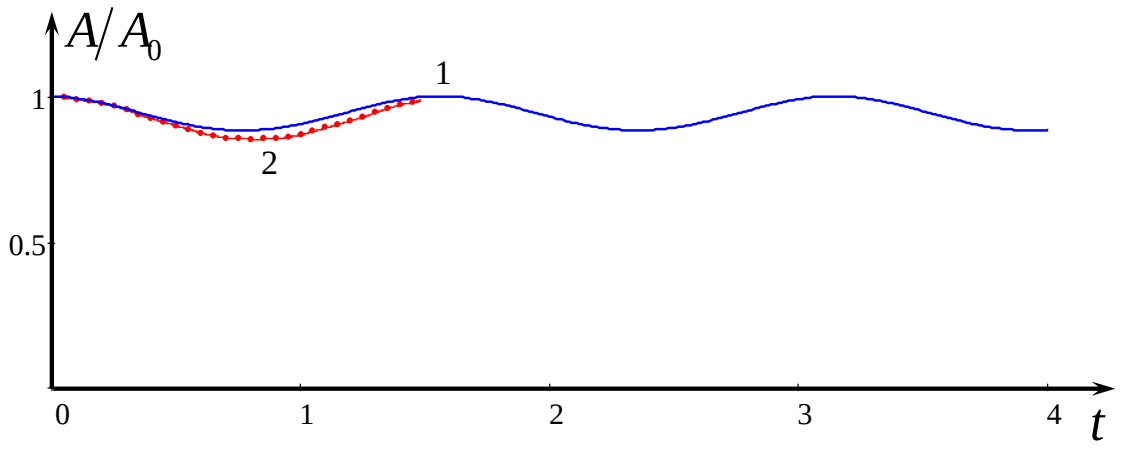

Figure 12 (colour online). Time dependence of normalised soliton amplitude. Line 1 – theoretical dependence; dots connected by line 2 represent the result of numerical computations.

It should be noted that the background wave is not an exact solution of the rotation modified BO equation (1). It is only an approximate solution when small scale dispersion is neglected. Therefore, in the process of evolution the background wave does not remain unchanged but varies slightly with time. However, at this relatively short time interval shown in Fig. 12 (within one period of soliton amplitude oscillation), the amplitude of the background wave remained practically constant. In addition, in the course of propagation the soliton produces trailing radiation due to the influence of large-scale dispersion [7]. The radiation interacts with the background wave and distorts it. This effect remains small if the amplitude of the background wave is relatively large compared with the amplitude of the radiation and the wavelength is much greater than the characteristic width of the soliton.

For another initial condition for the soliton amplitude $A = 1556$ and the same parameters for the sinusoidal wave, $U_0 = 15$ and $\Lambda = 100$, it was observed that the soliton does not oscillate around

the background wave trough, but drifts ahead and quickly escapes the wave period in which it was placed initially. This behaviour corresponds to one of black trajectories on the top of the phase plane in Fig. 4 for which the soliton amplitude is large enough that it cannot be captured by the background wave.

A further example for which the soliton amplitude is too small and so cannot be captured by the background wave is shown in Fig. 13. In this figure the soliton amplitude is $A = 32$, whereas the amplitude of the sinusoidal wave is $U_0 = 10$ and its wavelength is $\Lambda = 200$. The soliton was initially placed in the trough of the sinusoidal wave (see line 1 in Fig. 13) and gradually drifts back there (see lines 2, 3, … 9). This corresponds qualitatively to the portion of the phase trajectory 2 in Fig. 10 between $S = 0$ and $S = -5$. Eventually the soliton completely decays.

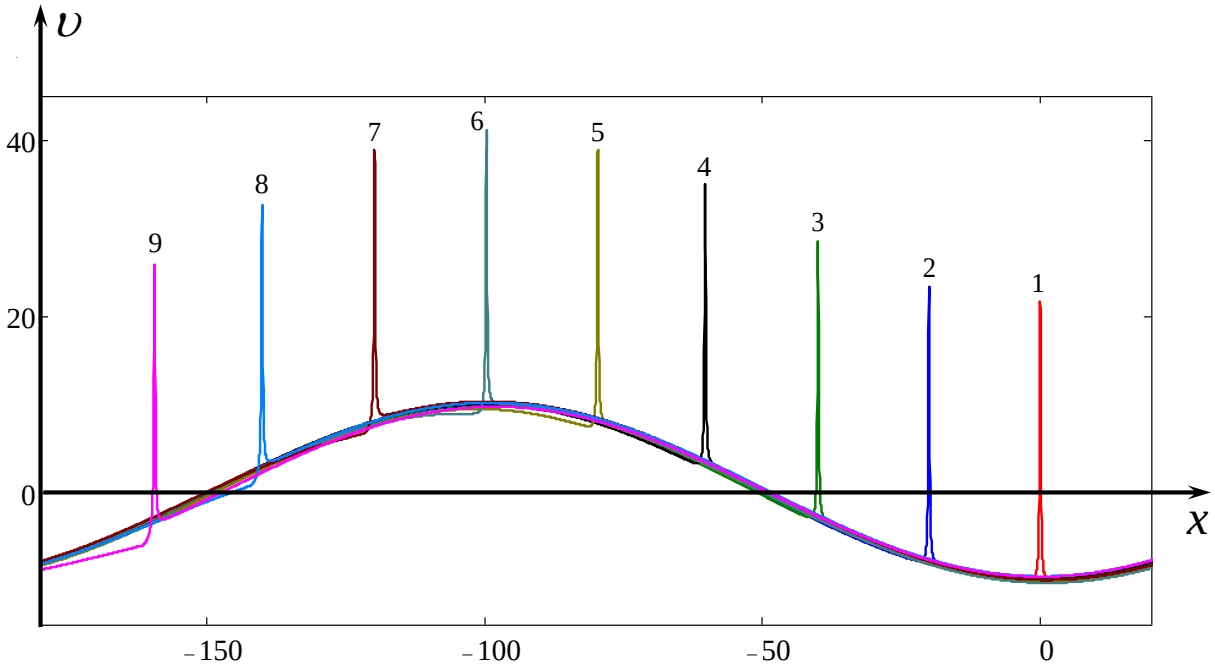

Figure 13 (colour online). A fragment of numerical solution of Eq. (1). Line 1 – the initial BO soliton located in the trough of the sinusoidal wave, other lines 2, 3, … 9 show solitons in the consecutive times in the coordinate frame co-moving with the sinusoidal wave.

5. Conclusion

In this paper, we have studied theoretically and numerically the process of interaction of an internal BO soliton with a long background wave in a rotating ocean. By means of an asymptotic analysis, we have derived a set of approximate equations (30)–(32) describing the amplitude and position of a soliton trapped in a background sinusoidal wave of small amplitude, as well as the

simultaneous variation of the amplitude of the background wave. The analysis of these equations shows that there are equilibrium positions for a soliton for which energy losses due to radiation caused by the rotation effect are compensated by energy pumping from the background wave. The soliton can experience decaying oscillations around the equilibrium position. However, the feedback of the soliton on the background wave eventually leads to the destruction of the coherent structure and energy dispersion in a quasi-random wave field. The theoretical results were validated by direct numerical modelling of the rotation modified BO equation (1). The agreement between the theory and numerical data are quite satisfactory within one period of the soliton oscillation around the equilibrium state at the trough of sinusoidal wave. Unfortunately, we were unable to produce a longer run due to the large amount of computation time required.

This study shows that long periodic waves on a pycnocline in the deep ocean can support quasi-stationary solitary waves co-propagating with the background wave and, possibly, oscillating around its troughs. Moreover, even more complicated structures consisting of several solitary waves within each period of a sinusoidal background wave, apparently, can exist which interact with each other. A similar problem has been studied within the Ostrovsky equation [23].

In conclusion, we can evaluate the range of applicability of the present theory to oceanic internal waves within the two-layer model. The coefficients of Eq. (1) in this case are given by Eq. (4). The wavelength of the background sinusoidal wave Λ in Eq. (1) should be large enough so that the short-wave dispersion term $\sim\beta$, can be neglected i.e. $\Lambda >> (\beta/\gamma)^{1/3}$. Choosing, for example, $(\rho_1 - \rho_0)/\rho_0 = 10^{-4}$, $h = 100$ m, and $f = 10^{-4}$ 1/s, we formally obtain $\Lambda >> 1$ km. This condition can be satisfied for internal waves with $\Lambda > 10$ km, which is not unrealistic for oceanic internal waves.

In this study the amplitude of the background wave was assumed to be small in comparison with the amplitude of the limiting wave, $U_0 << \beta/(36\alpha)$; in dimensionless form, $U_0 << U_{lim} \equiv \Lambda^2/36$. This condition was presented after Eq. (16). For near-surface internal waves this condition

reduces to the requirement $U_0 << \rho_1 h^2/108\rho_0$. Substituting the parameters indicated above, we obtain $U_0 << 10^2$ m.

We also assumed that the amplitude of the background wave U_0 is very small in comparison with the amplitude of a BO soliton, $U_0/A << 1$. This condition can be satisfied if we set $U_0 = 1$ m and $A = 10$ m. Then, the soliton width Δ should be much less compared with the background wavelength, $\Delta << \Lambda$, where $\Delta = 4\beta/\alpha A \approx 4h^2/3A \approx 1.3$ km, whereas $\Lambda \approx 10$ km.

In summary, the following parameters can be chosen for realistic oceanic conditions:

$\Lambda = 10$ km, $U_0 = 1$ m, $A = 10$ m and $\Delta = 1.3$ km.

The theory developed in this paper can shed light on fairly complicated process of the interaction of relatively small-scale solitary waves with large-scale tidal waves. One can expect that similar effects can occur within the rotation modified versions of the Gardner or Benjamin–Ono equations. Moreover, as shown in [23], the background wave can support not only a single soliton, but also several solitons interacting with each other, resulting in a steady wavetrain sitting at a certain phase of the periodic background wave. This issue deserves further study for applications to real physical systems, for which double dispersion (and corresponding double scale processes) can be realised.

Acknowledgments. Y.S. acknowledges the funding of this study from the State task program in the sphere of scientific activity of the Ministry of Science and Higher Education of the Russian Federation (project No. FSWE-2020-0007) and the grant of the President of the Russian Federation for state support of leading Scientific Schools of the Russian Federation (grant No. NSH-2485.2020.5).

References

1. L.A. Ostrovsky, Y.A. Stepanyants, Physica D 333 (2016) 266–275.
2. A.I. Leonov, Ann New York Acad. Sci. 373 (1981) 150–159.
3. V.M. Galkin, Yu.A. Stepanyants, J. Appl. Maths. Mechs. 55 (1991) 939–943.
4. T.B. Benjamin, J. Fluid Mech. 29 (1967) 559–592.
5. H. Ono, J. Phys. Soc. Japan, 40 (1976) 1487–1497.
6. R. Grimshaw, Stud. Appl. Math. 73 (1985) 1–33.
7. R. Grimshaw, N. Smyth, Y. Stepanyants, Wave Motion 78 (2018) 98–115.
8. O.A. Gilman, R. Grimshaw, Yu.A. Stepanyants, Stud. Appl. Math. 95 (1995) 115–126.
9. G.Y. Chen, J.P. Boyd, Physica D 155 (2001) 201–222.
10. J.P. Boyd, G.Y. Chen, Wave Motion 35 (2002) 141–155.
11. O.A. Gilman, R. Grimshaw, Yu.A. Stepanyants, Dynam. Atmos. and Oceans 23 (1996) 403–411.
12. L.A. Ostrovsky, Oceanology 18 (1978) 119–125.
13. L.A. Ostrovsky, Yu.A. Stepanyants, In Nonlinear Waves 3. Proc. 1989 Gorky School on Nonlinear Waves, eds A.V. Gaponov-Grekhov, M.I. Rabinovich and J. Engelbrecht. Springer-Verlag, Berlin–Heidelberg (1990) 106–128.
14. R.H.J. Grimshaw, L.A. Ostrovsky, V.I. Shrira, Yu.A. Stepanyants, Surveys in Geophys. 19 (1998) 289–338.
15. J.P. Boyd, Euro. J. Appl. Math. 16 (2005) 65–81.
16. Y.A. Stepanyants, Chaos, Solitons and Fractals 28 (2006) 193–204.
17. Ablowitz M. J., Segur H. Solitons and the Inverse Scattering Transform. 1981, SIAM, Philadelphia.
18. R.H.J. Grimshaw, J.-M. He, L.A. Ostrovsky, Stud. Appl. Math. 101 (1998) 197–210.
19. L.A. Ostrovsky, K.A. Gorshkov, In: P. Christiansen and M. Soerensen (eds.) Nonlinear science

at the down at the XXI century, Amsterdam, Elsevier. (2000) 47−65.

20. R. Grimshaw, K. Helfrich, Stud. Appl. Math. 121 (2008) 71–88.
21. M. Obregon, Y. Stepanyants, Math. Model. Natural Phenomena 7 (2012) 113–130.
22. K.A. Gorshkov, L.A. Ostrovsky, Physica D 3 (1981) 428−438.
23. L.A. Ostrovsky, Y. Stepanyants, Complex dynamics of solitons in rotating fluids. In: The Many Facets of Complexity Science, eds. D. Volchenkov, Springer, 2020.
24. B. Fornberg, G.B. Whitham, Phil. Trans. Roy. Soc. Lond. Ser. A: Math. Phys. Sci., 289 (1978) 373–404.
25. T.F. Chan, T. Kerkhoven, SIAM J. Numer. Anal., 22 (1985) 441–454.
26. L.N. Trefethen, Spectral Methods in MATLAB. 2000, SIAM, Philadephia.